



**HAL**  
open science

## **Countervailing vascular effects of rosiglitazone in high cardiovascular risk mice: Role of oxidative stress and PRMT-1**

Carmine Savoia, Talin Ebrahimian, Catherine A Lemarié, Pierre Paradis, Marc Iglarz, Farhad Amiri, Danesh Javeshghani, Ernesto L Schiffrin

### ► **To cite this version:**

Carmine Savoia, Talin Ebrahimian, Catherine A Lemarié, Pierre Paradis, Marc Iglarz, et al.. Countervailing vascular effects of rosiglitazone in high cardiovascular risk mice: Role of oxidative stress and PRMT-1. *Clinical Science*, 2010, 118 (9), pp.583-592. <10.1042/CS20090289>. <hal-00564472>

**HAL Id: hal-00564472**

**<https://hal.science/hal-00564472v1>**

Submitted on 9 Feb 2011

**HAL** is a multi-disciplinary open access archive for the deposit and dissemination of scientific research documents, whether they are published or not. The documents may come from teaching and research institutions in France or abroad, or from public or private research centers.

L'archive ouverte pluridisciplinaire **HAL**, est destinée au dépôt et à la diffusion de documents scientifiques de niveau recherche, publiés ou non, émanant des établissements d'enseignement et de recherche français ou étrangers, des laboratoires publics ou privés.



HAL Authorization

**Countervailing vascular effects of rosiglitazone in high cardiovascular risk mice:  
Role of oxidative stress and PRMT-1**

**Carmine Savoia MD<sup>1,3</sup>, Talin Ebrahimian PhD<sup>1</sup>, Catherine A Lemarié PhD<sup>1</sup>, Pierre Paradis PhD<sup>1</sup>, Marc Iglarz PhD<sup>1</sup>, Farhad Amiri PhD<sup>1</sup>, Danesh Javeshghani PhD<sup>1</sup>, Ernesto L Schiffrin MD, PhD, FRSC, FRCPC<sup>1,2</sup>**

<sup>1</sup>Lady Davis Institute for Medical Research and <sup>2</sup>Department of Medicine, Sir Mortimer B. Davis-Jewish General Hospital, McGill University, Montreal, QC, Canada, <sup>3</sup>Second Faculty of Medicine, Sapienza University of Rome and San Peter Hospital, Fatebenefratelli Research Center, Rome, Italy

**Word Count:** 5357; Abstract: 204; 7 figures.

**Key words:** hyperhomocysteinemia, rosiglitazone, atherosclerosis, endothelium, ADMA,

**Running title:** PPAR- $\gamma$  on vasculature in hyperhomocysteinemia plus high cholesterol

**Correspondence:**

Ernesto L. Schiffrin MD, PhD, FRSC, FRCPC  
Department of Medicine,  
SMBD-Jewish General Hospital, #B-127,  
3755 Côte-Ste-Catherine Rd, Montreal,  
Quebec, Canada H3T 1E2.  
E-mail: ernesto.schiffrin@mcgill.ca

## Abstract

We tested the hypothesis that the PPAR- $\gamma$  activator rosiglitazone improves vascular structure and function in aged hyperhomocysteinemic methylene tetrahydrofolate reductase gene (MTHFR) heterozygous knockout mice (*mthfr*<sup>+/-</sup>) fed a high cholesterol diet (HCD), a model of high cardiovascular risk. One year-old *mthfr*<sup>+/-</sup> were fed or not HCD (6 mg/Kg/day) and treated or not with rosiglitazone (20 mg/Kg/day) for 90 days, and compared to wild-type mice. Endothelium dependent relaxation of carotid arteries was significantly impaired (-40%) only in rosiglitazone treated HCD-fed *mthfr*<sup>+/-</sup>. Carotid media-to-lumen ratio (M/L) and cross-sectional area (CSA) were increased (2-fold) in *mthfr*<sup>+/-</sup> fed or not HCD compared to wild-type mice ( $P < 0.05$ ). Rosiglitazone reduced M/L and CSA only in *mthfr*<sup>+/-</sup> fed a normal diet. Superoxide production was increased in *mthfr*<sup>+/-</sup> fed HCD treated or not with rosiglitazone, whereas plasma nitrite was reduced by rosiglitazone in mice fed or not HCD. Protein arginine methyltransferase-1 (PRMT-1), involved in synthesis of the NO synthase inhibitor asymmetric dimethylarginine (ADMA), and ADMA were increased only in rosiglitazone-treated HCD-fed *mthfr*<sup>+/-</sup>. Rosiglitazone had both beneficial and deleterious vascular effects in this animal model of high cardiovascular risk: it prevented carotid remodeling, but impaired endothelial function in part through enhanced oxidative stress and increased ADMA production in mice at high cardiovascular risk.

## Introduction

Peroxisome proliferator-activated receptor  $\gamma$  (PPAR $\gamma$ ) belongs to a family of ligand-activated nuclear receptor and transcription factors which have been extensively studied in adipocytes [1,2,4], where they are involved in fat cell differentiation and lipid storage. PPAR $\gamma$  are present as well in liver and skeletal muscle, other targets of insulin action [1-3], and modulate insulin sensitivity in all these tissues. Rosiglitazone is a high-affinity ligand for PPAR $\gamma$  belonging to the thiazolidinedione (TZD) or glitazone class of synthetic compounds clinically used in the treatment of type-2 diabetes mellitus [1,4]. TZDs promote fatty acid oxidation and enhance insulin sensitivity in liver and skeletal muscle in part through inhibition of agents from adipose tissue that promote insulin resistance [5]. PPAR $\gamma$  is expressed in cardiovascular tissues, including heart, endothelium, vascular smooth muscle cells, and monocytes/macrophages [1].

*In vivo* and *in vitro* studies have demonstrated that, independently of metabolic effects, PPAR $\gamma$  activators exert anti-proliferative, antioxidant and anti-inflammatory effects on the cardiovascular system, and that they may be anti-atherogenic [1,4-10]. Hence, this class of drugs may represent a therapeutic tool for vascular protection and prevention of progression of atherosclerosis and cardiovascular disease. However, experimental and clinical studies have provided controversial results on the role of TZDs in the prevention of cardiovascular events in diabetic patients, who are at high cardiovascular risk [11]. Hyperhomocysteinemia (H-Hcy) is an independent risk factor for coronary, cerebral, and peripheral atherosclerosis [12,13]. Cardiovascular risk associated with H-Hcy is particularly high when combined with other risk factors (i.e. diabetes mellitus, high cholesterol, hypertension). Methylene tetrahydrofolate reductase (MTHFR) is a key enzyme in the remethylation cycle of homocysteine, which is converted to methionine [12]. A murine model of MTHFR deficiency, leading to increased plasma levels of homocysteine, develops atherosclerosis and vascular dysfunction when exposed to a high cholesterol diet (HCD) [14]. This model mimics a common cause of mild H-Hcy in humans [15,16]. We hypothesized that chronic administration of rosiglitazone would improve vascular structure and function in *mthfr* knockout mice fed HCD.

## Methods

### Animal Experiments

The study protocol was approved by the Animal Care Committee of the Lady Davis Institute and conducted in accordance with recommendations of the Canadian Council of Animal Care. Mice heterozygous for disruption of the *mthfr* gene presenting mild hyperhomocysteinemia were generated at the Montreal Children's Hospital Research Institute as already reported [14]. Heterozygous *mthfr*-deficient mice (*mthfr*<sup>+/-</sup>) and wild type controls were obtained by mating *mthfr*<sup>+/-</sup> mice with wild type BALB/cAnNCrIBR (Charles River, St-Constant, Qc, Canada). Old adult female *mthfr*<sup>+/-</sup> (n=24 divided in 4 groups as mentioned below) and wild type (n=6) littermate mice aged 11-12 months were studied. Homozygous mice have high mortality or delayed development and cerebellar abnormalities [14], and for this reason could not be studied. Heterozygous mice were divided into four groups (6 mice per group) fed or not HCD (6 mg/Kg/day; cholesterol 12.5 g/Kg; Research Diets #D12336, New Brunswick, NJ, USA), and treated or not with rosiglitazone (20 mg/Kg/day) for 90 days. Mice were sacrificed by CO<sub>2</sub> asphyxiation.

### Measurement of plasma cholesterol

Blood samples from the mice were collected in tubes containing EDTA. Plasma was separated by centrifugation and stored at  $-80^{\circ}\text{C}$ . Total plasma cholesterol was measured by enzymatic reaction.

### Evaluation of PPAR $\gamma$ expression

Snap-frozen aorta at level of the coronary sinus was pulverized in lysis buffer (2 mM EDTA; 1 mM EGTA; with protease inhibitors: 1  $\mu\text{g}/\text{mL}$  aprotinin, 1  $\mu\text{g}/\text{mL}$  leupeptin, 1  $\mu\text{g}/\text{mL}$  pepstatin, 1 mM PMSF, 1 mM  $\text{Na}_3\text{VO}_4$ ). Thereafter, samples were briefly sonicated and centrifuged (16000 g,  $4^{\circ}\text{C}$ , 30 min). Four  $\mu\text{g}$  of sample in a total incubation volume of 20  $\mu\text{l}$  as per manufacturer instructions was analyzed with an ELISA based kit (Active Motif, Carlsbad, CA, USA).

### Study of internal carotid arteries

Internal carotid arteries (2-3 mm in length) were placed in cold physiological salt solution containing (mmol/L) NaCl 120,  $\text{NaHCO}_3$  25, KCl 4.7,  $\text{KH}_2\text{PO}_4$  1.18,  $\text{MgSO}_4$  1.18,  $\text{CaCl}_2$  2.5, EDTA 0.026, and glucose 5.5. They were mounted on 2-glass microcannulae in a pressurized myograph. Endothelium-dependent relaxation was assessed by measuring the dilatory responses to acetylcholine ( $10^{-9}$  to  $10^{-4}$  mol/L) in vessels pre-contracted with norepinephrine ( $5 \times 10^{-5}$  mol/L). Endothelium-independent relaxation was assessed by the dilatory response to sodium nitroprusside ( $10^{-8}$  to  $10^{-4}$  mol/L). To evaluate nitric oxide (NO) availability, the concentration-response curve to acetylcholine was determined before and after 30-minute pre-incubation with the NO synthase (NOS) inhibitor N-nitro-L-arginine methyl ester (L-NAME,  $10^{-4}$  mol/L). Vessels were deactivated by perfusion with  $\text{Ca}^{++}$ -free physiological salt solution containing 10 mmol/L EGTA for 30 minutes. Lumen and media were measured at an intraluminal pressure at 60 mm Hg as previously described [17].

### Plasma nitrite measurement

Plasma nitrite as an index of NO production was evaluated with a colorimetric assay as previously described [18]. Duplicate samples of plasma (50  $\mu\text{l}$ ) were incubated with cadmium overnight at  $4^{\circ}\text{C}$  with gentle shaking. Plasma was mixed with 0.01% N-(1-naphtyl) ethylenediamine followed by mixing with 0.1% p-aminobenzenesulfonamide and total nitrite was determined by measuring absorbance at 548 nm.

### Plasma ADMA measurement

Blood samples were centrifuged at 3000 rpm for 10min at  $4^{\circ}\text{C}$  immediately after collection. Plasma samples were kept frozen at  $-80^{\circ}\text{C}$  until analysis. Twenty  $\mu\text{l}$  of plasma as per manufacturer's instructions were analyzed by an ELISA-based kit (DLD Diagnostika GmbH, Hamburg, Germany).

Accepted Manuscript

### Oxidative fluorescent microtopography

The oxidative fluorescent dye dihydroethidium (DHE) was used to evaluate *in situ* production of superoxide [19]. Unfixed frozen ring segments of aorta embedded in OCT were cut into 5-10  $\mu\text{m}$ -thick sections and placed on a glass slide. DHE ( $2 \times 10^{-6}$  mol/L) was topically applied to each tissue section. Slides were incubated in a light-protected humidified chamber at 37°C for 30 minutes and then coverslipped [20]. Images were obtained with a Leica fluorescent microscope. The amount of DHE staining present in the vessel wall was quantified (Northern Eclipse program, EMPIX Imaging Inc., Mississauga, ON, Canada) and expressed as percentage of the DHE fluorescence per total surface area.

### Western blot analysis for protein arginine methyltransferase (PRMT-1)

Protein was extracted from the coronary sinus area of snap frozen aorta as previously described [21]. Protein (100  $\mu\text{g}$ ) was separated by electrophoresis on 10% polyacrylamide gel and transferred onto a nitrocellulose membrane. Non-specific binding sites were blocked with 5% skimmed milk in Tris-buffered saline solution with Tween for 1 h at 24°C. Membranes were incubated overnight with anti-PRMT-1 polyclonal antibody (1:1000; Cell Signaling Technology, Danvers, MA). After incubation with the second antibody, the signal were revealed with chemiluminescence, visualized by autoradiography, and quantified densitometrically.

### In silico analysis of the PRMT-1 promoter.

The mouse PRMT-1 gene was examined *in silico* using UCSC genome bioinformatics Web site [22,23]. The 52238857-52242238 bp region of chromosome 7 was analyzed *in silico* using rVista to determine conserved PPAR $\gamma$  and PPAR response elements between mouse and human [24,25].

### Data analysis

Data are presented as mean  $\pm$  SEM. Morphological data were compared by ANOVA followed by Student–Newman–Keuls *post-hoc* test. Statistical evaluation of mechanical parameters was performed by repeated-measures ANOVA. A value of  $P < 0.05$  was considered statistically significant.

### Results

Mice with haploinsufficiency in MTHFR presenting mild hyperhomocysteinemia [14], were treated or not with HCD with or without rosiglitazone. Wild type littermate was used as control. Plasma cholesterol (Figure 1a) was similar in all the animals fed the normal diet and increased as expected in *mthfr*<sup>+/-</sup> mice fed HCD compared to wild type mice ( $P < 0.001$ ), and was significantly reduced after rosiglitazone treatment ( $P < 0.05$  vs. *mthfr*<sup>+/-</sup> fed HCD). In *mthfr*<sup>+/-</sup> mice fed a normal diet, the expression level of PPAR $\gamma$  in aorta was similar to wild type mice (Figure 1b). In *mthfr*<sup>+/-</sup> mice fed HCD, PPAR $\gamma$  expression was significantly increased compared to wild type mice ( $P < 0.05$ ). Rosiglitazone treatment induced a further increase in PPAR $\gamma$  expression in *mthfr*<sup>+/-</sup> mice fed HCD compared to untreated *mthfr*<sup>+/-</sup> mice fed HCD ( $P < 0.05$ ).

The M/L ratio of internal carotid arteries was similar in *mthfr*<sup>+/-</sup> mice fed normal diet compared to *mthfr*<sup>+/-</sup> mice fed HCD, and in both groups M/L was significantly greater than in wild type mice ( $P < 0.001$ , Figure 2). M/L ratio and media cross-sectional area (CSA) were significantly smaller after rosiglitazone treatment only in *mthfr*<sup>+/-</sup> mice compared to untreated *mthfr*<sup>+/-</sup> mice when both groups were fed normal diet ( $P < 0.01$  and  $P < 0.05$  respectively). However, hypertrophic remodelling was not improved by rosiglitazone treatment of *mthfr*<sup>+/-</sup> mice fed HCD.

Endothelium-dependent relaxation of carotid arteries was similar in *mthfr*<sup>+/-</sup> mice fed normal diet compared to wild type mice (Figure 3a), and was not different from *mthfr*<sup>+/-</sup> mice fed HCD or *mthfr*<sup>+/-</sup> mice fed the normal diet and treated with rosiglitazone. Vasodilation of carotid arteries in response to acetylcholine was significantly attenuated in *mthfr*<sup>+/-</sup> mice treated with rosiglitazone and fed HCD compared to HCD-fed *mthfr*<sup>+/-</sup> mice that did not receive rosiglitazone ( $P < 0.05$ ). Endothelium-independent relaxation was similar in all groups (Figure 3b). The NO synthase

inhibitor L-NAME significantly reduced acetylcholine-induced dilation in all groups (Figure 3c). In carotid arteries from rosiglitazone-treated *mthfr*<sup>+/-</sup> fed HCD, acetylcholine-induced dilation was only slightly inhibited by L-NAME (Figure 3d), indicating poor NO synthesis or bioavailability. Superoxide generation in carotid arteries was higher in *mthfr*<sup>+/-</sup> mice fed normal diet compared to wild type mice ( $P < 0.01$ , Figure 4). A further increase was observed in *mthfr*<sup>+/-</sup> mice fed HCD in comparison to *mthfr*<sup>+/-</sup> mice fed normal diet ( $P < 0.01$ ). Rosiglitazone did not affect superoxide production in carotid arteries of *mthfr*<sup>+/-</sup> mice fed normal or HCD. Plasma nitrite, an index of systemic NO production, was similar in *mthfr*<sup>+/-</sup> mice fed the normal or HCD compared to the wild type group. Rosiglitazone significantly reduced plasma nitrite concentration in both treatment groups (Figure 5a). Plasma levels of ADMA, an endogenous inhibitor of endothelial NO synthase (eNOS), were similar in *mthfr*<sup>+/-</sup> mice fed normal or HCD. Significantly elevated plasma ADMA levels were found in HCD fed *mthfr*<sup>+/-</sup> mice treated with rosiglitazone ( $P < 0.05$ ) (Figure 5b). The expression of PRMT-1, a key enzyme in the synthesis of ADMA, was similar in *mthfr*<sup>+/-</sup> mice compared to wild type mice independently of the diet. Rosiglitazone significantly enhanced PRMT-1 expression only in HCD-fed *mthfr*<sup>+/-</sup> (Figure 6).

The analysis of *prmt1* gene with the UCSC genome bioinformatics Web site revealed that it is contained on chromosome 7 and has four different alternative mRNA PRMT-1 splices (Figure 7b). The 52238857-52242238 bp region of chromosome 7 containing the two 5' exons and promoter region of the *prmt1* gene was analyzed using the rVista software, and several PPAR $\gamma$  response elements conserved between mouse and human were found (Figure 7a,c). The UCSC genome browser revealed that several regions of the PRMT-1 promoter are highly conserved among several mammalian species (Figure 7d).

## Discussion

Major findings from the present study of mild hyperhomocysteinemic *mthfr*<sup>+/-</sup> mice demonstrate that: 1) rosiglitazone improved vascular remodeling of carotid arteries, in part by reducing plasma cholesterol levels in mice fed HCD; 2) PPAR $\gamma$  agonism was associated with impaired endothelial function in the carotid arteries of *mthfr*<sup>+/-</sup> mice fed HCD, associated with decreased plasma nitrite and enhanced PRMT-1 expression and plasma levels of ADMA, an endogenous eNOS inhibitor; 3) rosiglitazone failed to reduce increased levels of reactive oxygen species (ROS) in *mthfr*<sup>+/-</sup> mice.

The association of several risk factors in a single individual is frequent in Western societies, and contributes to the development of atherosclerosis and cardiovascular dysfunction. Age, hypercholesterolemia and H-Hcy may participate in the progression of atherosclerosis, in part by inducing oxidative stress, endothelial dysfunction and inflammation [26,27]. This is the case for the murine model of mild atherosclerosis studied here, which is characterized by advanced age, mild H-Hcy, and elevated plasma cholesterol secondary to HCD. PPAR $\gamma$  activators exert pleiotropic effects on a wide range of tissues beyond their actions on insulin-responsive organs and tissues. These actions include inhibition of mechanisms that contribute to the progression of atherosclerosis [1,28]. TZDs may induce anti-atherogenic effects via different mechanisms, including the normalization of total plasma cholesterol, as shown in rats fed HCD [29], or via direct anti-inflammatory, anti-oxidant, and anti-hypertrophic effects [1,30-32], which may be independent of their metabolic actions. As expected [14], rosiglitazone reduced the lipid deposition found in the aorta of *mthfr*<sup>+/-</sup> mice (data not shown), potentially via reduction of plasma cholesterol in the mice fed HCD. Inflammatory markers such as VCAM-1 and osteopontin, which were increased in *mthfr*<sup>+/-</sup> mice, were only slightly decreased by rosiglitazone (data not shown), suggesting that PPAR $\gamma$  agonism did not have a marked anti-inflammatory effect in this particular model. PPAR $\gamma$  agonists block cell proliferation and enhance apoptosis of vascular smooth muscle cells [33,34] suggesting a role of TZDs in the modulation of vascular remodeling. Growth and migration of vascular smooth muscle cells into the intima is a central step of atherosclerotic plaque formation [35]. Hence, rosiglitazone may reduce atherosclerotic lesions in part by improving the vascular remodeling [36]. Rosiglitazone

attenuated intimal hyperplasia after arterial balloon catheter injury in a rat model of diet-induced H-Hcy, which presented a three-fold increase in proliferation of rat aortic vascular smooth muscle cells [37]. In persons with impaired glucose tolerance and no diabetes and cardiovascular disease, rosiglitazone modestly reduced carotid intima-media thickness [38], suggesting anti-atherogenic effects of PPAR $\gamma$  activation occurring particularly via remodeling of the vascular wall in humans. However, in type-2 diabetic patients, rosiglitazone had no significant effect on carotid atheroma as assessed by 3D carotid magnetic resonance imaging [39].

Endothelial dysfunction contributes to the development of atherosclerotic lesions and vascular remodeling, and its presence and severity is predictive of adverse outcomes [40]. Several cardiovascular risk factors may contribute to endothelial dysfunction, including age and hypercholesterolemia, by promoting vascular oxidative stress and impaired NO generation or bioavailability [26,27]. In particular, rabbits fed HCD had reduced NO levels and increased ADMA, an L-arginine analogue that acts as a competitive inhibitor of eNOS [41]. We recently reported that mesenteric arteries of young *methfr*<sup>+/-</sup> mice presented endothelial dysfunction due to increased oxidative stress and uncoupling of eNOS [42]. However, the precise mechanisms whereby H-Hcy produces endothelial dysfunction are incompletely defined. Besides decreased NO bioavailability due to increased ROS production, another potential mechanism for reduced NO effects in subjects with H-Hcy is decreased NO production due to increased levels of ADMA, [43]. Homocysteine reduces the catabolism and induces the synthesis of ADMA, the latter partially dependent on PRMT-1 activation [44]. Acetylcholine-induced vasodilation of carotid arteries from old *methfr*<sup>+/-</sup> was similar to that of age-matched wild type mice, and was 30% less than that observed in mesenteric arteries of younger mice [42]. It is possible that increased levels of homocysteine do not induce further impairment of endothelial function in addition to age-related endothelial dysfunction, despite the elevation of ROS levels in aorta of old *methfr*<sup>+/-</sup> mice.

Rosiglitazone, which reduced oxidative stress in young *methfr*<sup>+/-</sup> [42], did not reduce increased ROS production in old *methfr*<sup>+/-</sup> mice or improve endothelial function in these mice. Rosiglitazone treatment paradoxically resulted in greater impairment of endothelial function in *methfr*<sup>+/-</sup> mice fed HCD. It has been recently reported that homocysteine competes for PPAR nuclear receptors with PPAR agonists and may impair the maximum activation of PPAR receptors by the latter. Thus, homocysteine elevation may have an important impact on PPAR agonist action [45]. Furthermore, reduced production of NO, plus increased scavenging by excess ROS, may contribute to explain these results. Indeed, *methfr*<sup>+/-</sup> mice fed HCD presented the highest levels of ROS in aorta possibly due to the combined effect of age, high plasma cholesterol and H-Hcy. The endothelial dysfunction of HCD-fed *methfr*<sup>+/-</sup> treated with rosiglitazone may also explain the absence of improvement of vascular remodeling in this group despite a favourable effect on lipid deposition in atherosclerotic lesions. This suggests a countervailing effect of TZDs on progression of atherosclerosis depending on how many risk factors are contemporaneously present. Interestingly, HCD-fed *methfr*<sup>+/-</sup> mice treated with rosiglitazone presented increased expression of PPAR $\gamma$ , which has been recently reported to contribute to rosiglitazone-induced cardiotoxic effects [46].

An intriguing finding was that PRMT-1 was increased in rosiglitazone-treated HCD-fed *methfr*<sup>+/-</sup> mice. PRMT-1 is the major source of ADMA in the vasculature [43] and is partially activated by H-Hcy [42,46] as well as by LDL cholesterol [47]. The promoter of *prmt1* contains PPAR- $\gamma$  responsive elements which are highly conserved as shown in figure 7. Consistently with this finding, ADMA levels were increased approximately 2-fold in rosiglitazone-treated HCD-fed *methfr*<sup>+/-</sup> mice. Thus, rosiglitazone via increased expression and therefore activity of PRMT-1 leading to production of ADMA may decrease NO production and promote endothelial dysfunction in HCD-fed old *methfr*<sup>+/-</sup> mice, which already present high ROS generation in the vascular wall, thus amplifying this detrimental effect of H-Hcy and HCD.

These observations may support and extend results of recent experimental and clinical studies that challenge the vascular protective role of PPAR $\gamma$  activators in cardiovascular disease. TZDs have adverse effects on advanced atherosclerosis by promoting plaque instability [48], and PPAR $\gamma$  activation may contribute to monocytes differentiation into foam cells [49]. In humans, a recent

meta-analysis of rosiglitazone treatment trials in diabetic patients has shown that rosiglitazone may be associated with increased risk of myocardial infarction and death from cardiovascular cause [50], although methodological limitations do not allow definitive conclusions and this conclusion remains highly controversial. As a result, there is a situation of equipoise regarding the safety of rosiglitazone until further data is obtained [51].

### Clinical perspectives

Important new findings from this study are that rosiglitazone may exert beneficial and detrimental effects on the cardiovascular system depending on pre-existing levels of cardiovascular risk. Rosiglitazone exerted vascular protective effects in old mice with H-Hcy by attenuating vascular remodeling as well as the atherosclerotic process. However, it was unable to reduce the increased oxidative stress in *mthfr*<sup>+/-</sup> mice fed or not HCD, and exerted minimal effect on inflammatory mediators in these mice. When these mice became hypercholesterolemic in addition to aged and H-Hcy, the prior beneficial effect was counterbalanced by rosiglitazone-induced endothelial dysfunction, which may contribute to cardiovascular remodeling as well as to blunt any beneficial effect on atherosclerosis. These findings are consistent with current evidence for a role of PPAR $\gamma$  at the interface between the environment and control of metabolism [52]. Indeed, a common genetic variant of PPAR $\gamma$  in humans induces opposing effects on lipid and glucose metabolism depending on whether individuals are obese or sedentary, and depending on the fat composition of the diet [53]. In conclusion, the present study suggests mechanisms that may explain beneficial effects of PPAR $\gamma$  activation in lower risk subjects but detrimental actions in presence of high cardiovascular risk, which could explain some recent clinical observations in diabetic patients with advanced atherosclerosis.

### Acknowledgments

The authors thank André Turgeon for his excellent technical work. This work was supported by grant 82790 from the Canadian Institutes of Health Research (CIHR), the Canada Research Chair (CRC) Program of CIHR/Government of Canada, and the Canada Fund for Innovation (CFI), all to ELS, and a fellowship from the Heart and Stroke Foundation to TE and CAL.

### Disclosures

No conflicts to disclose.

## References

1. Touyz, R., and Schiffrin, E.L. (2006) Peroxisome proliferator-activated receptors in vascular biology-molecular mechanisms and clinical implications. *Vascul. Pharmacol.* **45**(1),19-28
2. Tontonoz, P., Hu, E., and Spiegelman, B.M. (1994) Stimulation of adipogenesis in fibroblasts by PPAR $\gamma$ , a lipid-activated transcription factor. *Cell* **79**,1147–1156
3. Olefsky, J.M., and Saltiel, A.R. (2000) PPAR gamma and the treatment of insulin resistance. *Trends. Endocrinol. Metab.* **11**,362–368
4. Duan, S.Z., Usher, M.G., and Mortensen, R.M. (2008) Peroxisome proliferators-activated receptor- $\gamma$ -mediated effects in the vasculature. *Circ. Res.* **102**,283-294
5. Evans, R.M., Barish, G.D., and Wang, Y.X. (2004) PPARs and the complex journey to obesity. *J. Nat. Med.* **10**(4),355-361
6. Tontonoz, P., Nagy, L., Alvarez, J.G., Thomazy, V.A., and Evans, R.M. (1998) PPAR $\gamma$  promotes monocyte/macrophage differentiation and uptake of oxidized LDL. *Cell.* **93**,241-252
7. Marx, N., Sukhova, G.M., Murphy, C., Libby, P., and Plutzky, J. (1998) Macrophages in human atheroma contain PPARgamma: Differentiation-dependent PPARgamma expression and reduction of MMP-9 activity through PPARgamma activation in mononuclear phagocytes in vitro. *Am. J. Pathol.* **153**,17-23
8. Ricote, M., Huang, J., Fajas, L., Li, A., Welch, J., Najib, J., Witztum, J.L., Auwerx, J., Palinski, W., and Glass, C.K. (1998) Expression of the peroxisome proliferator-activated receptor  $\gamma$  (PPARgamma) in human atherosclerosis and regulation in macrophages by colony stimulating factors and oxidized low density lipoprotein. *Proc. Natl. Acad. Sci. USA.* **95**,7614-7619
9. Staels, B., Koenig, W., Habib, A., Merval, R., Lebret, M., Pineda-Torra, I., Delerive, P., Fadel, A., Chinetti, G., Fruchart, J.C., Najib, J., Maclouf, J., and Tedgui, A. (1998) Activation of human aortic smooth-muscle cells is inhibited by PPAR $\alpha$  but not by PPAR $\gamma$  activators. *Nature.* **393**,790-793
10. Chinetti, G., Gbaguidi, G.F., Griglio, S., Mallat, Z., Antonucci, M., Poulain, P., Chapman, J., Fruchart, J.C., Tedgui, A., Najib-Fruchart, J., and Staels, B. (2000) CLA-1/SR-BI is expressed in atherosclerotic lesion macrophages and regulated by activators of peroxisome proliferator-activated receptors. *Circulation.* **10**,2411-2417
11. Robinson, J.G. (2008) Should we use PPAR agonists to reduce cardiovascular risk? *PPAR Res.* **28**,891425
12. Welch, G.N., and Loscalzo, J. (1998) Homocysteine and atherothrombosis. *N. Engl. J. Med.* **338**,1042-1050
13. Eikelboom, J.W., Lonn, E., Genest, J. Jr., Hankey, G., and Yusuf, S. (1999) Homocysteine and cardiovascular disease: a critical review of the epidemiologic evidence. *Ann. Intern. Med.* **131**,363-375
14. Chen, Z., Karaplis, A.C., Ackerman, S.L., Pogribny, I.P., Melnyk, S., Lussier-Cacan, S., Chen, M.F., Pai, A., John, S.W., Smith, R.S., Bottiglieri, T., Bagley, P., Selhub, J., Rudnicki, M.A., James, S.J., and Rozen, R. (2001) Mice deficient in methylenetetrahydrofolate reductase exhibit hyperhomocysteinemia and decreased methylation capacity, with neuropathology and aortic lipid deposition. *Hum. Mol. Genet.* **10**,433-443
15. Kang, S.S., Zhou, J., Wong, P.W., Kowalysyn, J., and Strokosch, G. (1998) Intermediate homocysteine: a thermolabile variant of methylenetetrahydrofolate reductase. *Am. J. Hum. Genet.* **43**,414-421
16. Frosst, P., Blom, H.J., Milos, R., Goyette, P., Sheppard, C.A., Matthews, R.G., Boers, G.J., van den Heijer, M., Kluijtmans, L.A., and van den Heuvel, L.P. (1995) A candidate genetic

- risk factor for vascular diseases: a common mutation in methylenetetrahydrofolate reductase. *Nat. Gen.* **10**,111-113
17. Neves, M.F., Endemann, D., Amiri, F., Viridis, A., Pu, Q., Rozen, R., Schiffrin, E.L. (2004) Small artery mechanics in hyperhomocysteinemic mice: effects of angiotensin II. *J Hypertens.* **22**(5):959-966
  18. Javeshghani, D., Sairam, R.M., Schiffrin, E.L., and Touyz R.M. (2007) Increased blood pressure, vascular inflammation, and endothelial dysfunction in androgen-deficient follitropin receptor knockout male mice. *J.A.S.H.* **1**(5),353-361
  19. Rothe, G., and Valet, G. (1990) Flow cytometric analysis of respiratory burst activity in phagocytes with hydroethidine and 2',7'-dichlorofluorescein. *J. Leukoc. Biol.* **47**,440-448
  20. Miller, F.J. Jr., Gutterman, D.D., Rios, C.D., Heistad, D.D., and Davidson, B.L. (1998) Superoxide production in vascular smooth muscle contributes to oxidative stress and impaired relaxation in atherosclerosis. *Circ. Res.* **82**(12),1298-305
  21. Savoia, C., Ebrahimian, T., He, Y., Gratton, J.P., Schiffrin, E.L., and Touyz, R.M. (2006) Angiotensin II/AT2 receptor-induced vasodilation in stroke-prone spontaneously hypertensive rats involves nitric oxide and cGMP-dependent protein kinase. *J. Hypertens.* **24**,2417-2422
  22. Kent, W.J., Sugnet, C.W., Furey, T.S., Roskin, K.M., Pringle, T.H., Zahler, A.M., Haussler, D. (2002) The human genome browser at UCSC. *Genome. Res.* **12**(6):996-1006
  23. <http://genome.ucsc.edu/>
  24. Loots, G., Ovcharenko, I., Pachter, L., Dubchak, I., Rubin, E. (2002) rVISTA for comparative sequence-based discovery of functional transcription factor binding sites. *Genome. Res.* **12**:832-839
  25. <http://genome.lbl.gov/vista/index.shtml>
  26. Savoia, C., and Schiffrin, E.L. (2006) Inhibition of the renin angiotensin system: implications for the endothelium. *Curr. Diab. Rep.* **6**,274-278
  27. Touyz, R., and Schiffrin, E.L. (2004) Reactive oxygen species in vascular biology: implications in hypertension. *Histochem. Cell. Biol.* **122**,339-352
  28. Heikkinen, S., Auwerx, J., and Argmann, C.A. (2007) PPAR $\gamma$  in human and mouse physiology. *Biochim. Biophys. Acta.* **1771** (8),999-1013
  29. Schaalán, M., El-Abhar, S., Maged, B., and El-Deshary, E.S. (2009) Westernized-like-diet-fed rats: effect on glucose homeostasis, lipid profile, and adipocyte hormones and their modulation by rosiglitazone and glimepiride. *J. Diabetes Complications.* **23**(3),199-208
  30. Li, A.C., Brown, K.K., Silvestre, M.J., Wilson, T.M., Palinski, W., and Glass, C.K. (2000) Peroxisome proliferator-activated receptor  $\gamma$  ligands inhibit development of atherosclerosis in LDL-receptor knock-out mice. *J. Clin. Invest.* **106**,523-531
  31. Minamikawa, J., Tanaka, S., Yamauchi, M., Inoue, D., and Koshiyama, H. (1998) Potent inhibitory effect of troglitazone on carotid arterial wall thickness in type 2 diabetes. *J. Clin. Endocrinol. Metab.* **83**,1818-1820
  32. Chen, Z., Ishibashi, S., Perrey, S., Osuga, J., Gotoda, T., Kitamine, T., Tamura, Y, Okazaki, H., Yahagi, N., Iizuka, Y., Shionoiri, F., Ohashi, K., Harada, K., Shimano, H., Nagai, R., and Yamada, N. (2001) Troglitazone inhibits atherosclerosis in apolipoprotein E-20 knock-out mice: pleiotropic effect on CD36 expression and HDL. *Arterioscl. Thromb. Vasc. Biol.* **21**,372-377
  33. Marx, N., Schonbeck, U., Lazar, M.A., Libby, P., and Plutzky, J. (1998) Peroxisome proliferator activated receptor  $\gamma$  activators inhibit gene expression and migration in human vascular smooth cells. *Circ. Res.* **83**,1097-1103
  34. Bruemmer, D., Yin, F., Liu, J., Berger, J.P., Sakai, T., Blaschke, F., Fleck, E., Van Herle, A.J., Forman, B.M., and Law, R.E. (2003) Regulation of the growth arrest and DNA damage inducible gene 45 (GADD45) by peroxisome proliferator-activated receptor  $\gamma$  in vascular smooth muscle cells. *Circ. Res.* **93**,e38-e47
  35. Ross, R. (1999) Atherosclerosis-an inflammatory disease. *N. Engl. J. Med.* **340**,115-126.

36. Collins, A.R., Meehan, W.P., Kintscher, U., Jackson, S., Wakino, S., Noh, G., Palinski, W., Hsueh, W.A., and Law, R.E. (2001) Troglitazone inhibits formation of early atherosclerotic lesion in diabetic and non diabetic low density lipoprotein receptor deficient mice. *Arterioscl. Thromb. Vasc. Biol.* **21**,365-371
37. Murthy, S.N., Obregon, D.F., Chattergoon, N.N., Fonseca, N.A., Mondal, D., Dunne, J.B., Diez, J.G., Jeter, J.R., Jr., Kadowitz, P.J., Agrawal, K.C., McNamara, D.B., and Fonseca, V.A. (2005) Rosiglitazone reduces serum homocysteine levels, smooth muscle proliferation, and intimal hyperplasia in Sprague-Dawley rats fed high methionine diet. *Metab. Clin. Exper.* **54**,645-652
38. Lonn, E.M., Gerstein, H.C., Sheridan, P., Smith, S., Diaz, R., Mohan, V., Bosch, J., Yusuf, S., Dagenais, G.R.; DREAM (Diabetes REDuction Assessment with ramipril and rosiglitazone Medication) and STARR Investigators. (2009) Effect of ramipril and of rosiglitazone on carotid intima-media thickness in people with impaired glucose tolerance or impaired fasting glucose: STARR (STudy of Atherosclerosis with Ramipril and Rosiglitazone). *J. Am. Coll. Cardiol.* **53**,2028-2035.
39. Varghese, A., Yee, M.S., Chan, C.F., Crowe, L.A., Keenan, N.G., Johnston, D.G., Pennell, D.J. (2009) Effect of rosiglitazone on progression of atherosclerosis: insights using 3D carotid cardiovascular magnetic resonance. *J. Cardiovasc. Magn. Reson.* **11**,24-32.
40. Schachinger, V., Britten, M.B., and Zehier, A.M. (2000) Prognostic impact of coronary vasodilator dysfunction on adverse long-term outcome of coronary heart disease. *Circulation.* **101**,1899-1906
41. Bolayirli, I.M., Aslam, M., Balci, H., Altug, T., Hacibekiroglu, M., and Seven, A. (2007) Effects of atorvastatin therapy on hypercholesterolemic rabbits with respect to oxidative stress, nitric oxide pathway and homocysteine. *Life. Sci.* **81**(2),121-127
42. Virdis, A., Iglarz, M., Neves, M.F., Amiri, F., Touyz, R.M., Rozen, R., and Schiffrin, E.L. (2003) Effect of hyperhomocysteinemia and hypertension on endothelial function in methylene tetrahydrofolate reductase-deficient mice. *Arterioscl. Thromb. Vasc. Biol.* **23**,1352-1357
43. Valance, P., and Leiper, J. (2004) Cardiovascular biology of the asymmetric dimethylarginine: dimethylarginine dimethylaminohydrolase pathway. *Arterioscl. Thromb. Vasc. Biol.* **24**,1023-1030
44. Lentz, S.R., Rodinov, R.N., (2003) Dayal, S. Hyperhomocysteinemia, endothelial dysfunction, and cardiovascular risk: the potential role of ADMA. *Atherosclerosis.* **4**,61-65
45. Hayden, M.R. (2008) Homocysteine competes for the peroxisome proliferator-activated receptor nuclear receptors. *J. Cardiometab. Syndr.* **3**(1),70-71
46. Son, N.H., Park, T.S., Yamashita, H., Yokoyama, M., Huggins, L.A., Okajima, K., Homma, S., Szabo, M.J., Huang, L.S., and Goldberg, I.J. (2007) Cardiomyocyte expression of PPAR $\gamma$  leads to cardiac dysfunction in mice. *J. Clin. Invest.* **117**,2791-2801
47. Böger, R.H., Sydow, K., Borlak, J., Thum, T., Lenzen, H., Schubert, B., Tsikas, D., and Bode-Böger, S.M. (2000) LDL cholesterol upregulates synthesis of asymmetrical dimethylarginine in human endothelial cells: involvement of S-adenosyl methionine-dependent methyltransferases. *Circ. Res.* **87**(2),99-105
48. Thorp, E., Kuriakose, G., Shah, Y.M., Gonzalez, F.J., and Tabas, I. (2007) Pioglitazone increases macrophage apoptosis and plaque necrosis in advanced atherosclerotic lesions of non diabetic low-density lipoprotein receptor-null mice. *Circulation.* **116**,2182-2190
49. Tontonoz, P., Nagy, L., Alvarez, J.G., Thomazy, V.A., and Evans, R.M. (1998) PPAR $\gamma$  promotes monocyte/macrophage differentiation and uptake of oxidized LDL. *Cell.* **93**,241-252
50. Nissen, S.E., and Wolski, K. (2007) Effect of rosiglitazone on the risk of myocardial infarction and death from cardiovascular causes. *N. Engl. J. Med.* **356**,2457-2471
51. Psaty, B.M., and Furberg, C.D. (2007) Rosiglitazone and cardiovascular risk. *N. Engl. J. Med.* **356**,522-2524

52. Semple, R.K., Chatterjee, V.K., and O’Rahilly, S. (2006) PPAR gamma and human metabolic disease. *J. Clin. Invest.* **116**,581-589
53. Luan, J., Brawne, P.O., Harding, A.H., Halsall, D.J., O’Rahilly, S., Chatterjee, V.K., and Wareham, N.J. (2001) Evidence of gene-nutrient interaction at the PPAR gamma locus. *Diabetes.* **50**,686-689

Accepted Manuscript

THIS IS NOT THE VERSION OF RECORD - see doi:10.1042/CS20090289

## Figures legends

**Figure 1:** a) Plasma cholesterol levels in *methfr*<sup>+/-</sup> and wild type mice. b) Expression of PPAR $\gamma$  at level of the coronary sinus of aorta in *methfr*<sup>+/-</sup> and wild type mice. +/+ : wild type control mice; +/- : *methfr*<sup>+/-</sup> mice fed normal diet; +/- HCD: *methfr*<sup>+/-</sup> mice fed high cholesterol diet; +/- R: *methfr*<sup>+/-</sup> mice fed normal diet and treated with rosiglitazone; +/- HCD/R: *methfr*<sup>+/-</sup> mice fed high cholesterol diet and treated with rosiglitazone. \**P*<0.05.

**Figure 2:** Media-to-lumen ratio and media cross-sectional area (CSA) of the carotid from *methfr*<sup>+/-</sup> and wild type mice measured at 60 mm Hg intraluminal pressure. \**P*<0.05.

**Figure 3:** a) Concentration-response curve to acetylcholine (Ach) and b) to sodium nitroprusside (SNP) of norepinephrine-pre-contracted mesenteric resistance arteries from *methfr*<sup>+/-</sup> and wild type mice. c) and d) Concentration-response curve to acetylcholine  $\pm$  the nitric oxide synthase (NOS) inhibitor L-NAME. \**P*<0.05.

**Figure 4:** Dihydroethidium (DHE) staining (upper panel) of reactive oxygen species (ROS) in aorta of *methfr*<sup>+/-</sup> and wild type mice. ROS production was increased in the aorta of *methfr*<sup>+/-</sup> mice. \**P*<0.05; †*P*<0.05 vs. +/+, +/-, +/- R.

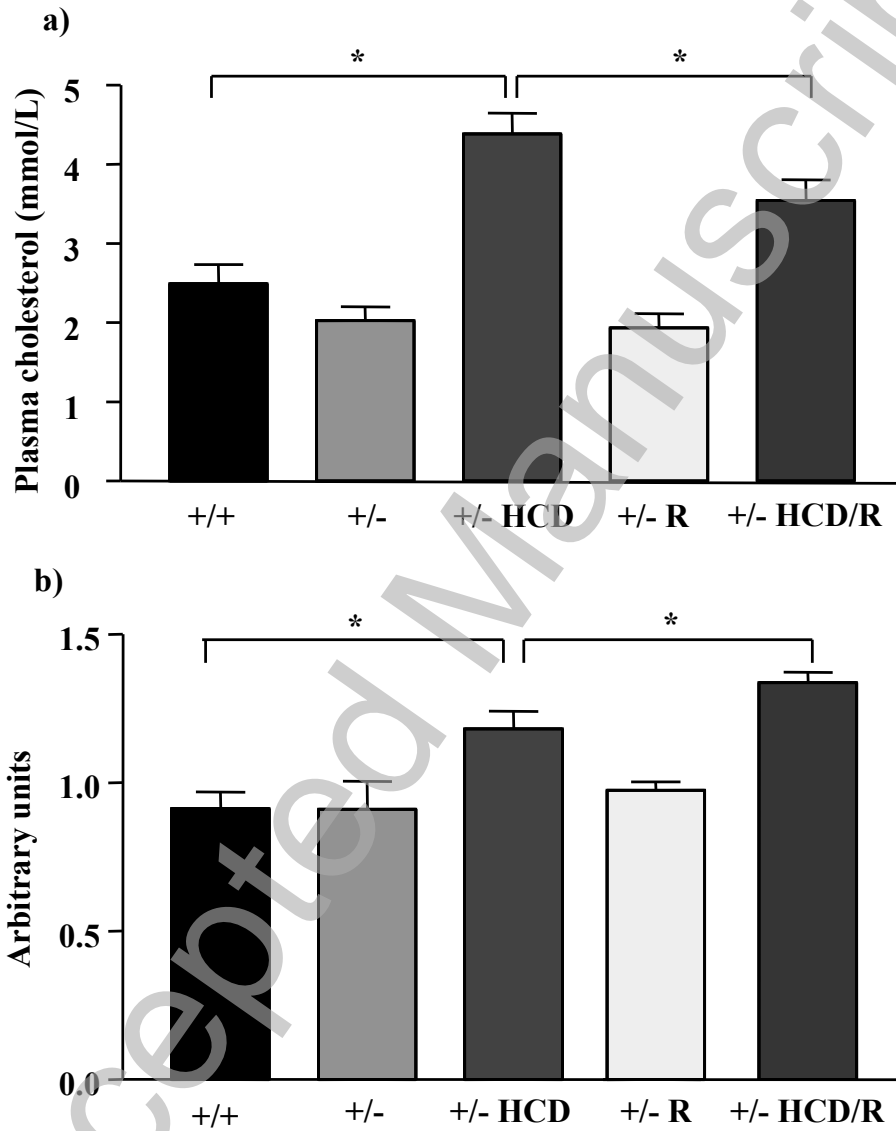
**Figure 5:** a) Plasma nitrite (index of NO production) in *methfr*<sup>+/-</sup> and wild type mice. b) Plasma concentration of the endogenous NOS inhibitor asymmetric dimethylarginine (ADMA) in *methfr*<sup>+/-</sup> mice. \**P*<0.05.

**Figure 6:** Protein arginine methyltransferase-1 (PRMT-1) expression in the aorta of *methfr*<sup>+/-</sup> mice. Results are presented as percentage of PRMT-1 expression in wild type control mice. \**P*<0.05.

**Figure 7:** In silico analysis of *prmt1* gene. The 52238857-52242238 bp region of chromosome 7 (a) containing the two 5' exons and the promoter region of the *prmt1* gene responsible for the transcription of four different alternative mRNA PRMT-1 splices (b) are presented. Coding and non-coding exons are indicated by wide black and narrow gray rectangles, respectively. Direction of the transcription is indicated by arrowheads and is from right to left. c) Conserved PPAR and PPAR $\gamma$  response elements between mouse and human are indicated. d) Several regions of the *prmt1* promoter that are highly conserved among mammals are displayed.

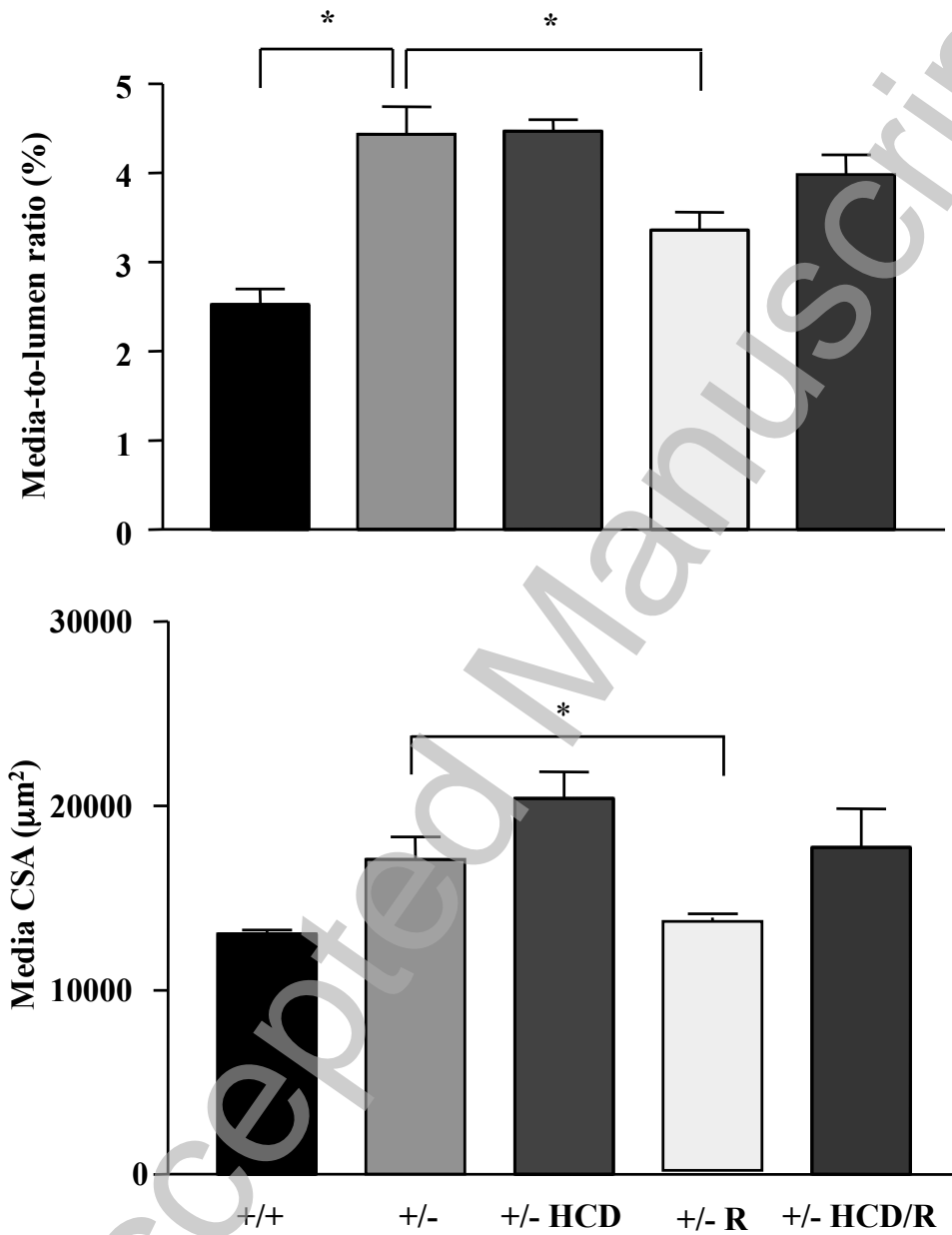
ACCEPTED MANUSCRIPT

Figure 1



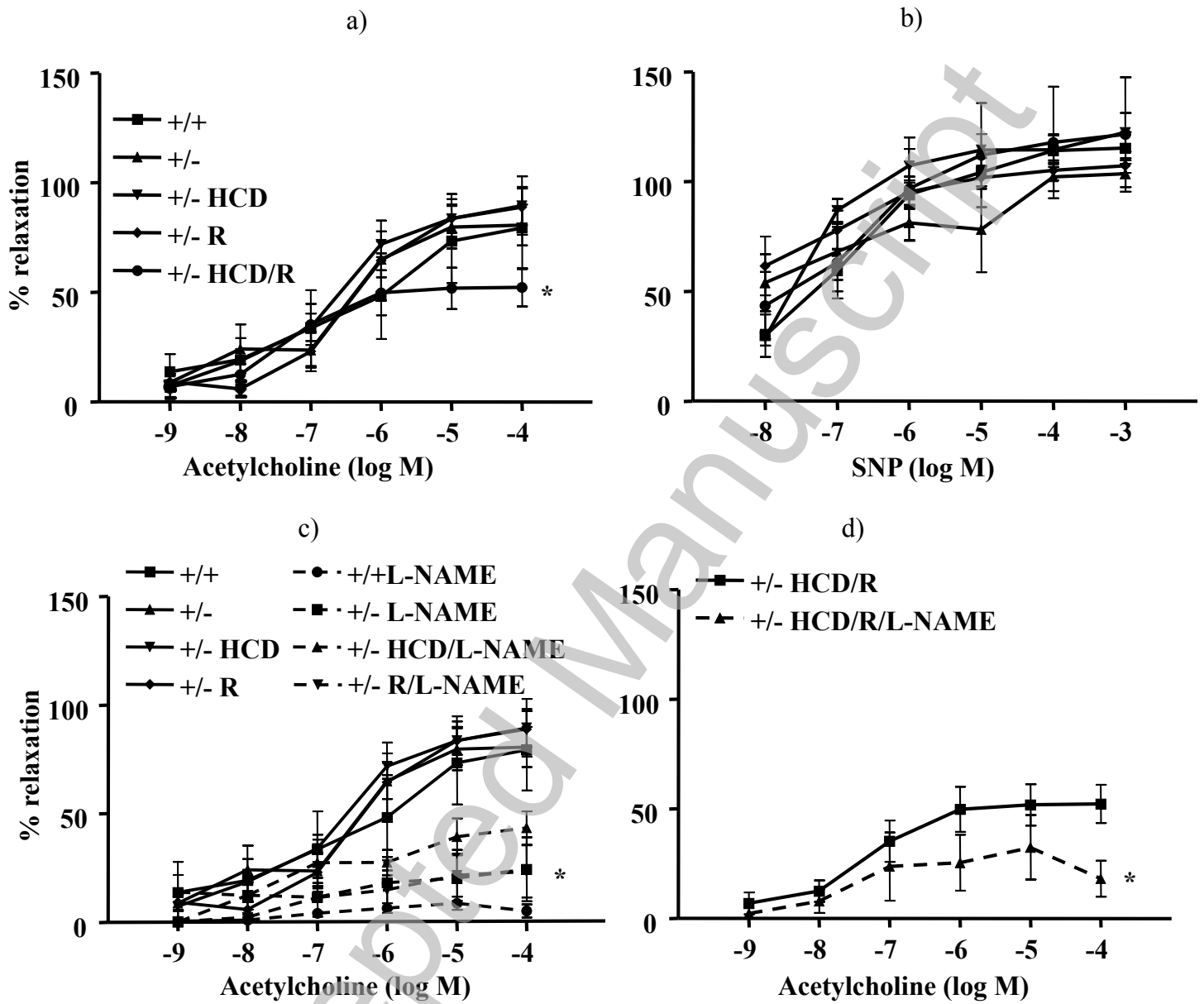
THIS IS NOT THE VERSION OF RECORD - see doi:10.1042/CS20090289

Figure 2



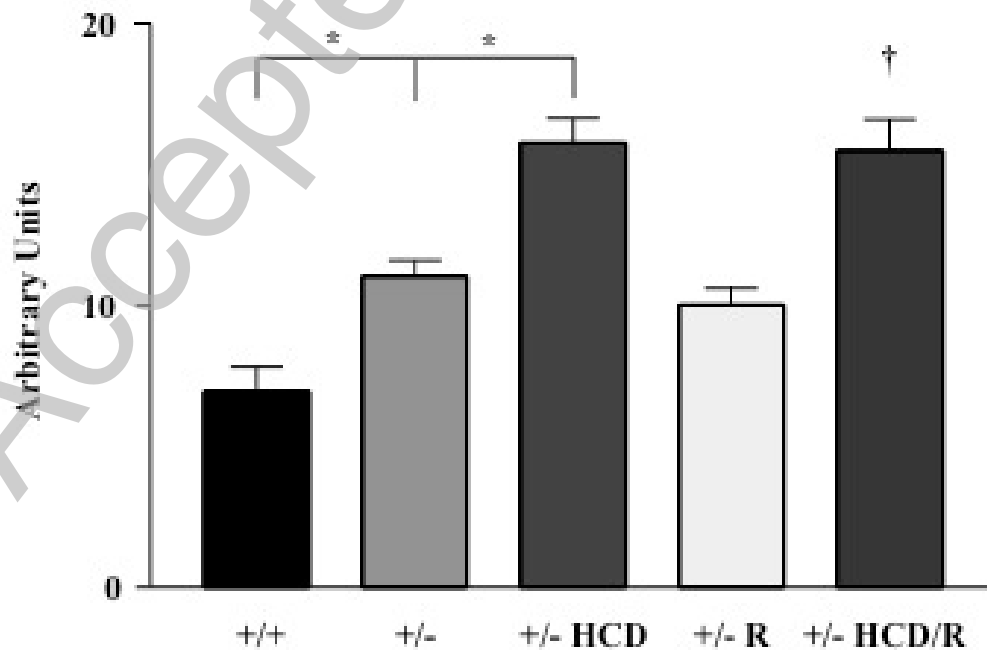
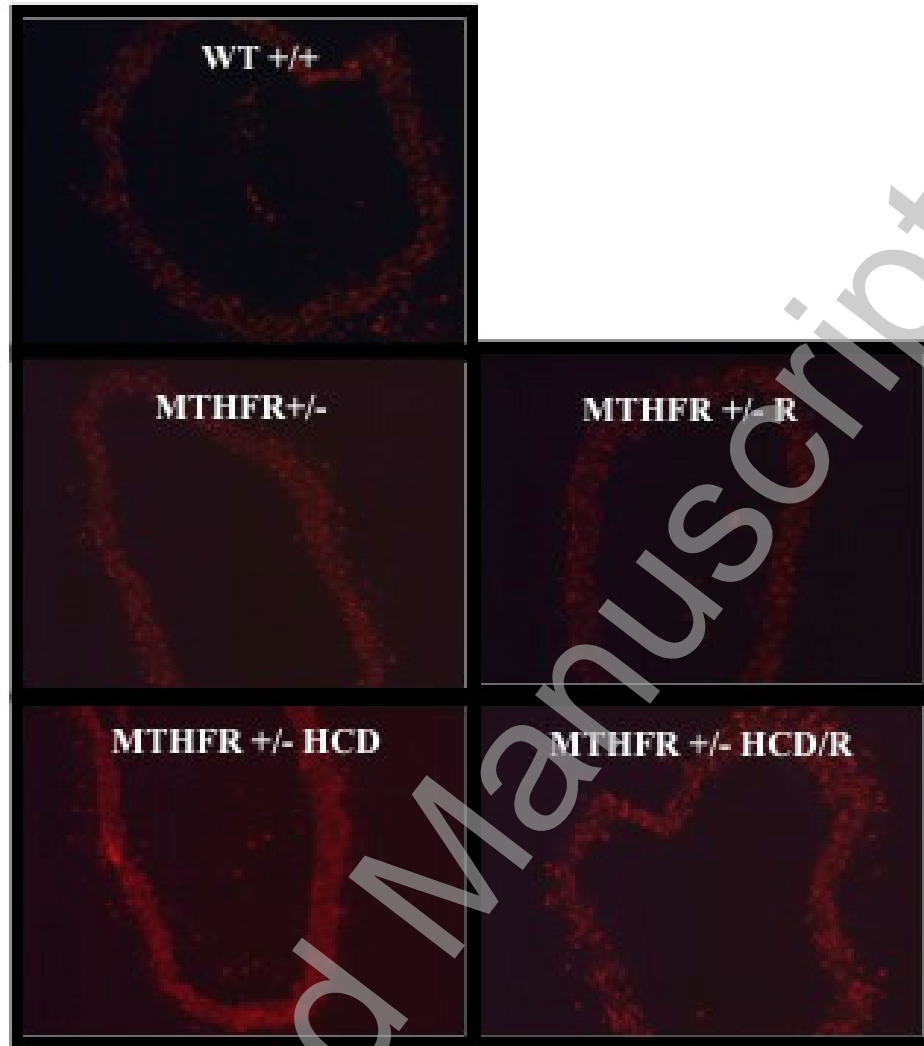
THIS IS NOT THE VERSION OF RECORD - see doi:10.1042/CS20090289

Figure 3



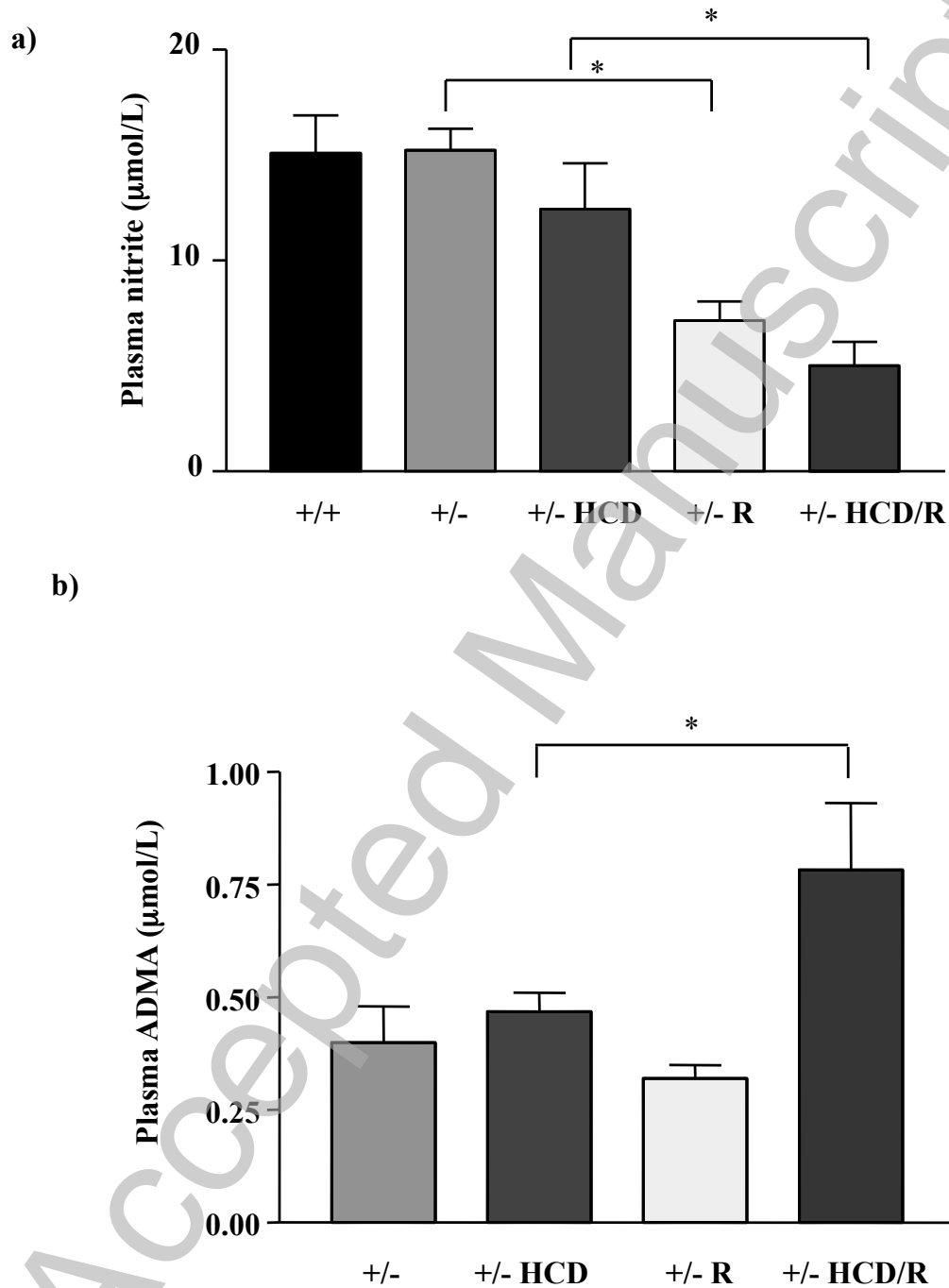
THIS IS NOT THE VERSION OF RECORD - see doi:10.1042/CS20090289

Figure 4



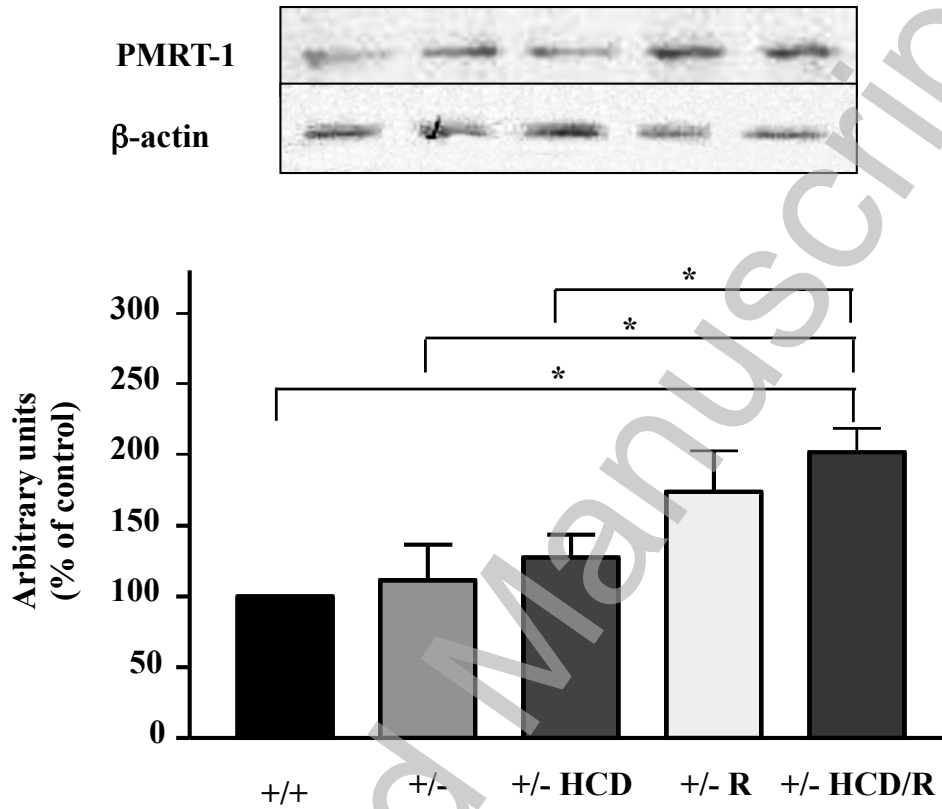
THIS IS NOT THE VERSION OF RECORD - see doi:10.1042/CS20090289

Figure 5



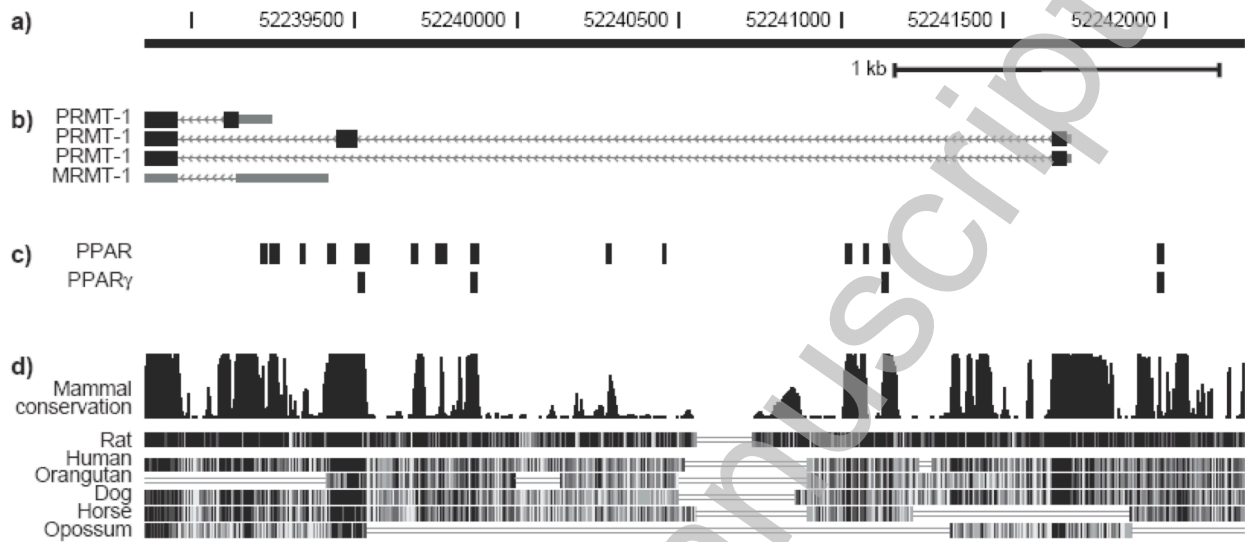
THIS IS NOT THE VERSION OF RECORD - see doi:10.1042/CS20090289

Figure 6



THIS IS NOT THE VERSION OF RECORD - see doi:10.1042/CS20090289

Figure 7



THIS IS NOT THE VERSION OF RECORD - see doi:10.1042/CS20090289

Accepted Manuscript